

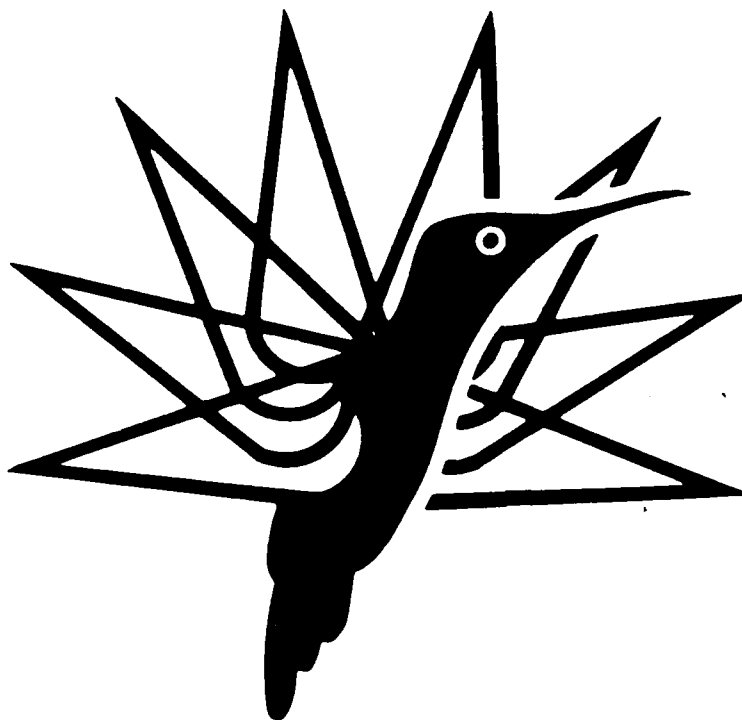
DTIC FILE COPY

PAPER Nr.: 86

1

DTIC  
ELECTE  
NOV 14 1989  
D S D

AD-A216 828



**TIME AND FREQUENCY-DOMAIN IDENTIFICATION AND VERIFICATION  
OF BO 105 DYNAMIC MODELS**

JÜRGEN KALETKA  
WOLFGANG VON GRÜNHAGEN

DEUTSCHE FORSCHUNGSANSTALT FÜR  
LUFT- UND RAUMFAHRT E.V. (DLR)  
INSTITUT FÜR FLUGMECHANIK  
D-3300 BRAUNSCHWEIG, FRG

MARK B. TISCHLER  
JAY W. FLETCHER

AEROFIGHTDYNAMICS DIRECTORATE  
US ARMY AVIATION RESEARCH  
AND TECHNOLOGY ACTIVITY  
AMES RESEARCH CENTER  
MOFFET FIELD, CALIFORNIA 94035-1099, USA

STATEMENT A  
Approved for public release  
Distribution Unlimited

**FIFTEENTH EUROPEAN ROTORCRAFT FORUM**

SEPTEMBER 12 - 15, 1989 AMSTERDAM

89 11 03 053

# TIME AND FREQUENCY-DOMAIN IDENTIFICATION AND VERIFICATION OF BO 105 DYNAMIC MODELS

Jürgen Kaletka  
Wolfgang von Grünhagen

Deutsche Forschungsanstalt für  
Luft- und Raumfahrt e.V. (DLR)  
Institut für Flugmechanik  
D-3300 Braunschweig, FRG

Mark B. Tischler  
Jay W. Fletcher

Aeroflightdynamics Directorate  
US Army Aviation Research  
and Technology Activity  
Ames Research Center  
Moffet Field, California 94035-1099, USA

## Abstract

Mathematical models for the dynamics of the DLR BO 105 helicopter are extracted from flight test data using two different approaches: frequency-domain and time-domain identification. Both approaches are reviewed. Results from an extensive data consistency analysis are given. Identifications for 6 degrees of freedom (DOF) rigid body models are presented and compared in detail. The extracted models compare favorably and their prediction capability is demonstrated in verification results. Approaches to extend the 6 DOF models are addressed and first results are presented.

## 1. Introduction

System identification is broadly defined as the deduction of system characteristics from measured data. It provides the only possibility to extract both non-parametric (e.g. frequency responses) and parametric (e.g. state space matrices) aircraft models from flight test data and therefore gives a reliable characterization of the dynamics of the actually existing aircraft. Main applications of system identification are seen in areas where higher accuracies of the mathematical models are required: Simulation validation, control system design (in particular model-following control system design for in-flight simulation), and handling qualities (Figure 1).

To investigate the efficiency of individual identification approaches, a dedicated flight test program was conducted with the DLR BO 105. The flight test data were provided as a data base to the AGARD Working Group FMP WG18 on *Rotorcraft System Identification*. In addition, the data were extensively evaluated by the DLR and US Army (both members in the AGARD WG) as part of an ongoing US/FRG Memorandum of Understanding (MOU) on *Helicopter Flight Control*. This joint effort in system identification is a continuation of the cooperation that started with the identification of the XV-15 Tilt Rotor aircraft [1].

The paper mainly concentrates on the identification and verification of conventional 6 degrees of freedom (DOF) rigid body derivative models. These models can accurately describe helicopter dynamics in the low and mid frequency range (eg. up to about 13 rad/sec for the BO 105). They are broadly applicable to many areas such as piloted-simulation, simulation validation, handling qualities, etc.. Application to high bandwidth flight control, however, requires higher order models that include the coupled rotor/body response. Therefore, the identification of extended models with an improved representation of the high frequency range is also addressed.

The paper first reviews the dynamics identification techniques, which have been developed in the US and the Federal Republic of Germany. The BO 105 data base is described and results from a data consistency analysis are discussed. Then, identification results for 6 DOF models obtained from both, US Army and DLR techniques, are presented and compared and verification results are shown. Finally, results from first approaches to extend the 6 DOF rigid body model are presented.

## 1. Overview of Identification Techniques

Depending on the considered system and the individual requirements various identification methodologies have been developed and applied. In general, they can be separated into two categories: time domain and frequency domain. Each of these approaches has its inherent strengths and weaknesses and requires the analyst's skill and experience for a successful application. Both, DLR and US Army have been developing their own methodol-



<input checked="" type="checkbox"/>
<input type="checkbox"/>
<input type="checkbox"/>
Codes
ed / or dial

A-1

ogies for aircraft system identification. DLR has gained extensive experience with time-domain identification techniques applied to both, fixed-wing and rotary-wing aircraft. Much of the experience with rotorcraft identification is associated with the DLR BO 105 helicopter to provide models for handling qualities and the control system design for in-flight simulation. The US Army has been concentrating on frequency-domain identification techniques in support of handling qualities, flight, and simulation experiments. Extensive experience with these techniques was obtained from the identification of the open-loop dynamics of the XV-15 Tilt Rotor. Further applications were associated with the Bell 214ST, UH60, and the US Army/NASA variable stability helicopter CH-47B.

### 1.1 Time-Domain Identification Method

The general approach used in aircraft system identification is shown in Figure 2. In flight tests, specifically designed control input signals are executed to excite the aircraft modes of interest. The inputs and the corresponding aircraft response are measured and recorded. A Least Squares identification technique is initially applied to the measured data to check their internal compatibility. Data inconsistencies resulting from e.g. calibration errors, drifts, or instrumentation failures are detected by comparing redundant measurements from independent sensors. This approach, which can be used on-line, helps to obtain the data quality required for system identification.

For the identification step, the aircraft dynamics are modeled by a set of differential equations describing the external forces and moments in terms of accelerations, state, and control variables, where the coefficients are the stability and control derivatives. The responses of the model and the aircraft resulting from the control inputs are then compared. The response differences are minimized by the identification algorithm that iteratively adjusts the model coefficients. In this sense, aircraft system identification implies the extraction of physically defined aerodynamic and flight mechanics parameters from flight test measurements. Usually, it is an off-line procedure as some skill and iteration are needed to select appropriate data, develop a suitable model formulation, identify the coefficients, and, finally, verify the results. Here, model formulation involves consideration of model structure, elimination of non-significant parameters, and inclusion of important nonlinearities. As the time-domain approach directly leads to parametric results in the form of state space models, model formulation is an important issue inasmuch as there are only a few tools that can provide some help. For the parameter estimation, a Maximum Likelihood technique is used that also allows a nonlinear model formulation [2]. As the identified model usually is obtained from a small number of flight tests, a model verification step is mandatory to prove its validity and its suitability for applications.

### 1.2 Frequency-Domain Identification Procedure

The frequency-domain identification procedure developed by the US Army/NASA is depicted in Figure 3. Pilot-generated frequency-sweep inputs are used to obtain broad-band excitation of the vehicle dynamics of interest. In the case of the BO 105, good excitation was achieved from 0.05 Hz - 5 Hz, which includes all of the important rigid body and rotor dynamic modes. A data compatibility analysis is completed using the Kalman filter/smoothing program SMACK. Measurement scale factors and biases are estimated, as well as reconstructed estimates of unknown states and/or noisy measurements. In the present case the body axis airspeeds (u,v,w) were estimated to remove the effects of rotor wake interference on the airspeed measurements. Results from SMACK are catalogued for identification processing by the package SIF (System Identification Facility), developed at the Ames Research Center. The key step in the frequency-domain identification procedure is the extraction of high-quality frequency responses between each input/output pair, using the Chirp-Z transform (an advanced FFT) and overlapped/windowed spectral averaging [3]. When multiple control inputs are present in the excitation (i.e. within a single run), as is the case in the BO 105 data and most other open-loop tests, the contaminating effects of partially correlated inputs must be removed. An inversion of the frequency-response matrix of all inputs to a single output is completed for each frequency point and again for each output. (For single input systems, or for cases in which no multi-input correlation exists, the conditioned frequency-responses are identical to the conventional single-input/single-output responses). Associated with each conditioned frequency-response is the partial coherence, which is a measure of the accuracy of the conditioned frequency-response identification at each frequency point. The resulting set of high-quality "conditioned frequency-responses" forms the key ingredient of the frequency-domain procedure.

For the frequency-domain method, the identification criterion is based on the weighted square-error between the measured and model frequency-responses (The prefixes "conditioned" and "partial" are omitted but are implied in all of the following references to "frequency-responses" and "coherence", respectively). The frequency-ranges for the identification criterion are selected individually for each input/output pair according to the overall range of good coherence. The weighting is based on the values of coherence at each frequency point to emphasize the most accurate data. The identification algorithm iteratively adjusts the stability and control derivatives and time delays in the model until convergence on a minimum error criterion is achieved. The direct identification of time delays is a key characteristic of the frequency-domain approach. Start-up values of the model used in the minimization algorithm may be obtained from one of three sources:

1. direct inversion of transfer-function model fits of the frequency-response data (as illustrated in [4]),
2. equation-error identification results,
3. a-priori values based on simulation models.

In the present case, a preliminary ML identification result obtained by the DLR was used, although a later analysis showed that the same converged solution was obtained when estimates were used from an equation-error identification (The equation-error method does not require start-up values so it is well suited for this purpose). Numerically linearized gradients of the identification criterion with respect to the model parameters is conducted to evaluate the sensitivity of the converged result to the included parameters, and to estimate parameter accuracy (Cramer-Rao lower bound). This information is used to "weed-out" those parameters, which are not important and to determine, which are highly correlated. The identification process is repeated on the reduced model structure until a final model with parameters having suitable Insensitivities ( $< 10\%$ ) and Cramer-Rao bounds ( $< 20\%$ ) are achieved or a significant rise occurs in the cost function [4]. The final model is verified by comparing predicted and measured responses for flight data not used in the identification. Applications of system identification results have included simulation validation [3], [4], handling-qualities specification testing [5], and flight-control system analyses [8].

## 2. Flight Test Data Base

A flight test program was conducted on a DLR BO 105 helicopter to obtain data especially designed for system identification purposes. Trim configuration was steady state horizontal flight at 80 knots in a density altitude of about 3000 feet. To avoid effects of atmospheric disturbances the tests were flown in practically absolutely calm air. Having established trim the pilot gave a prescribed input signal to one of the controls. To help him generating the input, a CRT was installed in the cockpit that showed both, the desired signal and the actual control movement. Taking flight tests with a longitudinal stick input as an example, Figure 4 shows that three basically different input signals were flown:

1. a modified multi-step 3211 signal with a total time length of 7 seconds. This signal, developed at DLR, has become standard in system identification as it excites a wide frequency band within a short time period. Therefore, it is particularly suited for slightly unstable systems when long duration tests cannot be flown without additional stabilization. Stabilization, however, should be avoided as it can cause significant identification difficulties due to output/input correlations. At the end of the input signal the controls were kept constant until the pilot had to retrim the aircraft.
2. frequency sweeps from about 0.08 Hz up to the highest frequency the pilot could generate (2 to 4 Hz, depending on the control). On the CRT the lowest frequency was shown as 'starting help'. Then the pilot progressively increased the frequency on his own. Since the input is pilot flown (and not computer generated) it is not purely sinusoidal and also contains input power below the starting frequency, thereby allowing lower frequency identification. Total time length of the sweeps was about 50 seconds, followed by the retrim of the aircraft to the initial steady state condition. Figure 4 shows that the input amplitudes are fairly constant. The pitch rate rapidly decreases at higher frequencies (with almost no response at the highest frequency), which shows that the rigid body motion could sufficiently be excited by pilot generated inputs.
3. doublet inputs, that can be considered as classical input signals for aircraft flight testing. For system identification, however, doublets are less suitable as they excite only a relatively small frequency band.

Within one test run only one control was used to excite the on-axis response and to avoid correlation with other controls. Because of the long time duration of the frequency sweeps, these tests required some stabilization by the pilot to keep the aircraft response within the limits of small perturbation assumptions for linear mathematical models. For redundancy reasons each signal was repeated at least three times.

In Figure 4 the roll- and pitch rate responses due to the three input signals are given in the same scales. It shows that the input amplitudes were adjusted to generate similar helicopter response magnitudes. It also demonstrates the highly coupled BO 105 characteristic: the (coupled) roll rate response due to a longitudinal stick input is as high as the primary pitch rate response.

Flight test data obtained from both the 3211 inputs and the frequency sweeps were used for the identification. These inputs have often shown their suitability for identification purposes. The multi-step inputs (3211) seem to be more appropriate for time-domain techniques whereas the frequency sweeps are better suited for the frequency-domain approach. Therefore, time-domain identification results (DLR) were obtained from the modified 3211 inputs. Frequency-domain identification results (US Army) are based on the frequency sweeps. The flight test data obtained from doublet control input signals were then used to verify the identified models.

### 3. Data Reliability Analysis

Measurements used for system identification included body angular rates, linear accelerations, attitude angles, speed components, and controls. They were mainly obtained from conventional sensors: rate and vertical gyros, accelerometers located close to the CG, and potentiometers at the pilot controls. Speed was measured by a HADS air data system, using a swiveling pitot static probe located below the main rotor. The measured data were sampled and recorded on board of the helicopter. As identification results are extremely sensitive to phase shift errors, emphasis was placed on the removal of analogue (anti-aliasing) filters. To still avoid aliasing errors, flight tests were conducted to define appropriate high sampling rates [7]. Further data processing steps included

1. data conversion to a unique sampling rate of 100 Hz,
2. measurement corrections for to the aircraft CG position, and
3. digital filtering to remove high frequency noise.

An absolute prerequisite for reliable system identification results is a high accuracy in the flight data measurements. To meet this requirement it is necessary to

1. check the data accuracy during the flight tests when the instrumentation can still be modified and calibrations can be corrected or repeated,
2. conduct a more detailed data quality analysis after the flight tests and, if necessary, correct the data before use for identification.

#### 3.1 Initial data check

In addition to standard quicklook plot evaluations, a computer supported data compatibility analysis was used. It allows to check the consistency between redundant measurements, like rates and attitude angles, during the flight test phase and to detect and eliminate instrumentation and calibration errors. This initial data check is based on a robust least-squares identification technique implemented on a microcomputer [8]. It has helped to improve the data measurement quality significantly and to drastically reduce the time and cost of flight tests with inaccurate and therefore unusable measurements.

#### 3.2 Data consistency analysis and data reconstruction

Data quality and consistency are critically important to the identification. Excessively noisy or kinematically inconsistent data may lead to identification of an incorrect model or inability to obtain convergence of the identification solution. Preliminary checks of data quality and consistency can ensure that these sources of error are minimized, therefore saving much time and effort in the identification process. Bad data can be replaced by conducting further flight tests or by reconstructing low quality measurements from other measured data.

A number of techniques are currently in use for performing data consistency/ state reconstruction calculations. These range in complexity from simple integration of the

equations of motion to the use of maximum likelihood estimators. For the present U.S. Army study the Kalman Filter Smoother program SMACK (Smoothing for AirCraft Kinematics) developed at the Ames Research Center was employed. The SMACK algorithm is based on a variational solution of a six-degree-of-freedom linear state and non-linear measurement model (Figure 5) and employs a forward smoother and zero-phase-shift backward information filter. The solution is iterative, providing improved state and measurement estimates until a minimum squared-error is achieved. Linearization is about a smoothed trajectory and convergence is quadratic [9].

Consistency checks were performed in two steps:

1. a preliminary 3 degree of freedom check including only the Euler angle and body angular rate measurements,
2. a final six-degree of freedom check including the angular variable measurements and the air-data and linear specific force measurements.

This approach allowed initial estimation of the angular-variable error parameters to be performed unbiased by the noisier air-data and specific-force measurements. The values estimated in the angular solution and their variances were then used as start-up values in the final overall solution. This two-step procedure resulted in a final solution with smaller parameter Cramer-Rao bounds and quicker convergence than a one-step coupled solution.

Before introduction into SMACK, the flight test data was preprocessed through a low-pass filter and a program to create companion arrays required by SMACK for the deweighting of bad data points. A zero-phase-shift low-pass filter with a cutoff frequency of 3Hz was used to reduce measurement noise associated with the high frequency vibrations. Estimates of one standard deviation of the measurement noises required by the Kalman Filter/Smoother were set equal to the resolution of the sensors, which were calculated from their dynamic ranges and the 12 bit ADC resolution. The validity of these estimates was confirmed by convergence of the program determined error covariances to values very close to the estimated noise intensities and the very "white" appearance of the residual time histories.

The velocity signals contained numerous "disturbances", which are due to interaction of the HADS air-data sensor with the rotor wake. To prevent these sections from biasing the SMACK solution incorrectly, they were deweighted using the companion arrays mentioned above. This had the effect of eliminating these points from the Kalman Filter measurement update.

Figure 6 illustrates typical improvements in the velocity time histories achieved with SMACK. The quality of the velocity frequency response identification was also increased. This can be seen from the comparison of the coherence functions for the identified  $V_{measured}/pedal$  and  $V_{reconstructed}/pedal$  frequency responses shown in Figure 7.

A further improvement in the velocity time histories is the elimination of a time lag in the measured velocity signals. This is quite evident in the comparison of measured and reconstructed lateral velocity in Figure 8. This discrepancy will cause identification results obtained from the measured velocity signals to differ from identification results based on the reconstructed velocity signals.

Table 1 contains a listing of the significant biases and scale factors identified for each of the 52 maneuvers as well as a statistical summary for each parameter. It can be seen that the most significant of these are the fairly large scale factors on  $v$  and  $w$ . Figure 6 illustrates how the 25% scale factor on  $v$  caused a 3 dB magnitude error in the  $v/pedal$  frequency response. Use of the measured lateral velocity signal created an inconsistency between the lateral velocity and lateral acceleration frequency responses, which initially prevented the frequency-domain identification from converging. However, when the reconstructed velocity signal was used instead, the identification was successful.

#### 4. Identification Results

Because of its rigid rotor system with a relatively high hinge offset the BO 105 helicopter response due to a control input is highly coupled in all degrees of freedom. Figure 4 already demonstrated the high roll response due to a longitudinal stick input. The classical modelling separation into longitudinal and lateral directional motions cannot be applied and at least a coupled 6 DOF rigid body model has to be used. For the identification it means that a larger number of parameters (in the order of 40 to 50 unknowns) must be determined. Therefore,

main effort must be placed on data information content, data quality, model structure, and a powerful evaluation technique.

This chapter will concentrate on results obtained for 6 DOF rigid body models.

#### 4.1 Time Domain Identification Results

As identification techniques fully rely on the measured input/output behaviour of the aircraft, the flight test data must contain sufficient information about the aircraft characteristics. Usually a single test run cannot meet this requirement. Therefore, different runs, individually flown, were concatenated to increase the data information content. From these runs, one common result is generated. An individual parameter can only be determined when it has an significant influence on the measured helicopter response. Inclusion of non-important parameters leads to the problem of model over-parameterization that can cause convergence problems and, due to parameter correlations, inaccurate estimates. Therefore, it is a very important step to carefully select the parameters to be identified and those to be omitted. For this model structure definition the parameter covariance matrix (Cramer-Rao lower bound) provided by the Maximum Likelihood identification technique proved to be a helpful tool. It was used to eliminate non-significant parameters and reduce high correlations between parameters. It must be mentioned that the covariance matrix is always based on the evaluated data set. Using other data can lead to different conclusions. The applied model structure was obtained from various data sets and, at least for multi-step inputs, proved to be quite consistent.

For the BO 105 Identification, four runs with 3211 inputs were selected for concatenation:

- one run with a longitudinal stick input,
- one run with a lateral stick input,
- one run with a pedal input,
- one run with a collective input.

The time duration for each run was 27 seconds. The state and measurement (observer) equations of the 6 DOF model are:

- State equations:  $\dot{x} = Ax + f(\text{kinematics}) + f(\text{gravity}) + Bu$
- Measurement equations:  $y = Cx + Du$
- State vector:  $x^T = (u, v, w, p, q, r, \Phi, \Theta)$
- Control vector:  $u^T = (\text{long stick, lat stick, pedal, collective})$
- Measurement vector:  $y^T = (a_x, a_y, a_z, u, v, w, p, q, r, \Phi, \Theta, \dot{p}, \dot{q}, \dot{r})$

Basically this model is linear. The equation terms due to kinematics and gravity forces were kept nonlinear and calculated using the actual states. No use was made of any pseudo control inputs (state variables are replaced by measurements and treated as additional control inputs). The rotational accelerations used in the measurement vector were digitally differentiated from the rate measurements. The measured speed components were used in the identification, although they are certainly the weakest part in the instrumentation as the sensor accuracy is only about 1 m/sec [11]. It was still felt that the speed information was usable and therefore was not replaced by reconstructed data, inasmuch as the linear accelerations were additionally used in the observer. It has however to be noted that this approach is different from the frequency-domain approach that uses reconstructed speed data.

When a control input is given, the model immediately generates an acceleration response. As an example, Figure 9 compares the roll accelerations due to a lateral stick input for a) the response of the identified model and b) the measured flight test data. It is clearly seen that the model response precedes the actual measurement. This time shift is mainly caused by the dynamic characteristics of two helicopter components that are not included in the model: the main rotor and the hydraulic system.

Unless the model is not extended by additional degrees of freedom, describing the hydraulic and rotor dynamics, their effect can only be approximated by equivalent time delays. Figure 9 also demonstrates that these delays can easily be determined by correlating model response and flight test data. For the discussed example, the highest value of the cross-correlation was obtained at a time delay of 60 milliseconds. Therefore, the lateral control input was delayed by 60 milliseconds and then the identification was repeated. The

improvement in the fit of the roll acceleration time histories is seen in the lower part of Figure 9

Using the cross-correlation approach, the following equivalent time delays were determined:

- roll acceleration/lateral stick: 60 msec
- pitch acceleration/long stick: 100 msec
- yaw acceleration/pedal: 60 msec
- vertical acceleration/collective: 40 msec
- pitch acceleration/collective: 100 msec

(For the identification, data with 50 samples/second were used. As time shifts are handled in multiples of the sampling interval, the above given delays are multiples of 20 milliseconds with a variance of 10 milliseconds.)

Significant time delay differences were seen in the collective response data. It already indicates that the equivalent time delay can be problematic and certainly is only a compromise when the rotor is not modelled. As two different time delays for one control can often not be applied, the time delay for the primary response, vertical acceleration, was chosen.

Figure 10 demonstrates, how important it is to include accurately defined equivalent time delays in the identification. Using two major derivatives, the roll damping  $L_p$  and the roll control derivative due to lateral stick, as an example, it shows the high sensitivity of the estimates to time delays (or phase shifts). A general measure of the identification quality is the determinant of the error covariance matrix, where the minimum of the determinant indicates the best possible fit between measurements and the model response. Figure 10 also shows that this minimum is reached at a time delay of about 60 to 80 milliseconds for the lateral stick, which is in agreement with the previous value of 60 milliseconds.

Using the above given time delays (40 msec for collective), the final identification results for the 6 DOF model were obtained. Time history comparisons for the measured and calculated rates are shown in Figure 11 and the identified derivatives are given in Table 2. The model gives a reliable representation of the BO 105 dynamics and, as it will be shown in the chapter on model verification, has a high predicting capability. As rotor DOF are only approximated by equivalent time delays, a decreasing model quality for higher frequencies must be expected. Such models are certainly appropriate and useful for applications in the lower frequency range, like handling qualities, simulation of the rigid body motion, etc..

#### 4.2 Frequency-Domain Identification Results

This section presents identification results obtained from the frequency-domain identification procedure. The conditioned frequency-response of roll rate/lateral stick obtained from 3 concatenated lateral stick sweeps is shown in (Figure 12a). The partial coherence for lateral stick inputs Figure 12b. Indicates excellent identification over a broad frequency range that includes the rigid body and rotor dynamics (0.6-23 rad/sec). Lower frequency identification ( $\omega < 0.6$  rad/sec) for lateral stick transfer-functions was hampered by the lack of sufficient low-frequency excitation for the lateral stick sweeps, as indicated by the falling partial coherence. However, good low-frequency pedal inputs were executed that allowed satisfactory identification of the low frequency dynamic modes. Partial coherence plots for the remaining controls shown in Figure 12c-e indicate that all controls contribute to the roll rate response, and must be included in the multivariable spectral analysis. In fact, the longitudinal input is nearly as significant as the lateral input for frequencies of about 1 rad/sec, which indicates considerable cross-control coupling. The multiple coherence of Figure 12f is nearly unity over a broad range, which indicates that the total roll rate power can be linearly accounted for by considering the 4 pilot inputs. This shows that turbulence and non-linear effects are not significant in this response. The conditioned frequency-response of Figure 12a is fairly flat over a broad frequency-range, as expected from the high value of  $L_p$  for the hingeless BO 105 rotor. The dip in magnitude in the frequency range of 2-3 rad/sec reflects the influence of the dutch roll mode. The resonance clearly visible at 15 rad/sec is the very lightly damped lead-lag/air-resonance mode. This mode is superimposed on the coupled body-roll/rotor-flapping response at 13.5 rad/sec.

Multivariable frequency-response identification was conducted on the remaining input/output pairs. In each case, the frequency-response was identified from the sweep that

corresponds to the respective input (i.e., the roll rate/longitudinal stick response was obtained from the longitudinal stick sweep). The set-up for the model identification is shown in Table 3. A total of 28 frequency-responses, with 19 frequencies in each, were matched in the iterative model identification process. The indicated relative weighting of phase vs. magnitude error is a commonly used value [3]. The frequency-range of fit was selected individually for each response corresponding to its range of good partial coherence; however, in all cases the upper frequency of the fit was limited to 13 rad/sec. This upper limit was enforced since the 6 DOF model is not capable of matching the lead-lag and coupled body/rotor flapping dynamics that dominate the response beyond this frequency. Without this restriction, the 6 DOF model structure can produce physically meaningless parameter values [10]. Further discussion of model structure considerations for high bandwidth applications is presented later.

The final results of the frequency-domain identification are listed in Table 2. As noted in the table, there are a number of parameters that were eliminated in the model structure determination phase. These parameters were found to be insensitive (i.e., unimportant to the frequency-response fits), or too highly correlated to be identified. These parameters were sequentially dropped, and the identification was repeated until the insensitivities and Cramer-Rao bounds were within satisfactory guidelines and just before a significant rise in the cost function was detected. For example, one parameter that could not be identified was the speed stability derivative,  $M_u$ . Analyses showed that this parameter was highly correlated with  $Z_u$ , resulting in an unacceptably large Cramer-Rao bound for  $M_u$  (98%). The source of this problem was the lack of sufficient low-frequency excitation in the longitudinal and collective sweep inputs. Another parameter,  $Y_{pedal}$ , was found to have an unacceptably large insensitivity (22.4%), which in turn yielded a large Cramer-Rao bound (85%). The large insensitivity means that this parameter does not significantly affect the frequency responses (and ultimately the cost function), and can be eliminated. For this forward flight condition, the side velocity and lateral acceleration responses to pedals ( $v_{pedal}$  and  $a_{pedal}$ ) are dominated by the yawing moment derivative  $N_{pedal}$ , except at very high frequencies outside of the range of the useable data. It is interesting to note that many of the parameters that were dropped in the model structure determination correspond to those that were dropped at the outset in the time-domain identification as being considered unimportant. However, other parameters, most notably the force derivatives ( $Y_p, Y_q, X_p, X_q$ ) which were excluded from the DLR model, were found to be important for matching the accelerometer responses.

Comparisons of the flight data and identified model frequency-responses are shown in Figure 13 for a number of characteristic responses. In these figures, only 50 frequency points are shown, which causes the data curves to display a more jagged appearance than the earlier response shown in Figure 13. In general, the agreement between the model and flight data is quite good, especially for the data, which has high coherence, and so is more heavily weighted in the identification.

## 5. Comparison of Results

Time and frequency-domain identification results are compared in this section in a number of formats:

1. parameter values,
2. eigenvalues,
3. frequency-responses.
4. time-response verification.

### 5.1 Comparison of parameter values

The stability and control derivatives, and time delays are listed for the two methods in Table 2. Overall agreement is quite good, especially considering that different flight data were used for the two methods. Significant differences are apparent only in three parameters ( $L_p, M_q$ , equivalent time delay for the collective), which are discussed in this section. The key source of the difference between the damping derivatives ( $L_p, M_q$ ) for the two identification results arises from the bandwidth of the data used in each approach. In the DLR time-domain method, the full bandwidth of the data was used, while in the frequency-domain method the data bandwidth was limited to 13 rad/sec. The frequency-domain identification was rerun with the full data bandwidth (data is good up to 30 rad/sec) and yielded  $L_p$  and  $M_q$  values of -10.16 rad/sec and -4.52 rad/sec, respectively, which are close to the DLR results. The sensitivity of the damping derivatives to data bandwidth indicates that the 6 DOF model structure

is inadequate for high-bandwidth identification. Extended model results are presented later in the paper, which address this issue.

The second difference in the results is the values for time delay for the collective input. The time-domain method for extracting time delay is based on evaluating the cross-correlation (time-domain equivalent to phase shift) of the on-axis (linear or angular) accelerations. The frequency-domain method searches for a time delay in conjunction with the other model parameters that will produce the best match of all of the responses (not just accelerations). The use of a single time delay for each input imposes the assumption that all input/output response pairs have the same high-frequency zeros, and thus the same high-frequency phase roll-off. This corresponds to modeling the rotor response as an actuator. When this assumption is valid, the two methods should produce essentially the same time delays, as they do for the lateral, longitudinal, and pedal inputs. However, this assumption is not acceptable for the collective inputs. Further frequency-domain analyses indicated an effective time delay of about 93 msec for linear responses ( $u$ ,  $w$ ,  $a_z$ ) to collective, but a much larger effective time delay of about 255 msec for angular responses ( $p$ ,  $q$ ). The time-domain result reflects the vertical acceleration delay, while the frequency-domain result reflects an average delay. Clearly a single average time delay value is not sufficient for characterizing all of the responses, and a higher-order dynamic model is needed.

## 5.2 Comparison of Eigenvalues

The eigenvalues for the two identification models are listed in Table 4. The previously discussed differences in  $L_p$  and  $M_q$  are reflected in associated differences in the first-order high-frequency roll and pitch modes. The remaining modes compare very favorably. The unstable phugoid mode ( $\omega = 0.33$  rad/sec for both methods) is a key aspect of the BO 105 handling-qualities for this flight condition.

## 5.3 Comparison of Frequency-Responses

Frequency-responses obtained from the DLR time-domain state-space models are compared with the previous frequency-domain identification results in Figure 13. The frequency-domain model fits the responses somewhat better as expected since the identification was based on these frequency-responses, and the DLR was extracted from different data (3211 inputs). Even so, the overall comparison is quite good. One exception is the frequency-response lateral acceleration/lateral stick Figure 13. The time-domain model shows a 20 dB/decade slope error in the high frequency magnitude response, and an attendant 90 deg phase shift. The cause for this discrepancy is the omission of the derivative  $Y_p$  in the time-domain model structure.

## 5.4 Time-Domain Verification and Comparison

Verification is a key final step in the system identification process that assesses the predictive quality of the extracted model. Flight data not used in the identification is selected in order to insure that the model is not tuned to specific data records or input forms. In this study, doublets inputs in each axis were used for model verification and comparison. Figure 14 compares the time response predictions of the two models for lateral and pedal doublets for all observer variables. As a further example, the roll and pitch axis responses are presented in Figure 15.

Overall, the predictive capability of both models is quite good in both the on- and off-axis responses, especially considering the dynamically-unstable and highly-coupled nature of the BO 105. As expected, the time-domain results fits the data somewhat better as it was derived from multi-step type inputs. Although there are still some small discrepancies, the overall agreement is quite satisfactory. The total squared-error for the models are in the same order showing that the overall correlation is of essentially the same quality. A few differences between the models' responses are worth noting. Speed data were treated differently in the two approaches. DLR used the measured data after a correction of the initial condition ( $v_0$  was set zero and, because of the horizontal trim flight condition,  $w_0$  was determined from the pitch angle  $\Theta$ ). The US Army used fully reconstructed speed data, as described in Chapter 3.2. The differences in the model responses are however so small that a final preference for one of these approaches cannot be made. The linear accelerations are fitted slightly better by the frequency-domain model due to fact that the force equations contain more parameters. Critical aspects in the speed and acceleration comparisons are also certainly due to the speed measurement problems together with the fact that helicopter acceleration measure-

ments are always deteriorated by high amplitude 'coloured' vibration noise leading to an unfavorable low signal/noise ratio.

## 8. Higher-Order Model Identification

Six DOF models can only describe the rigid body motion. For most fixed wing aircraft such models have become standard and, depending on the applications, models for subsystems, like the control system or the engine, are sometimes added. For helicopters, however, the main rotor who has a dominant effect on the motion, is not explicitly modeled. Based on the assumption that the rotor dynamics are at significantly higher frequencies than the body modes, they are neglected and the rotor influence is lumped into the rigid body derivatives. As response to a control input, such a model assumes an instantaneous tilt of the tip path plane and an immediate helicopter angular acceleration. Figure 9 has already demonstrated that this approximation yields less accurate results for the initial (or higher frequency) response and that it is at least necessary to represent the effect of the rotor dynamics by equivalent time delays.

The results of the previous sections indicate that coupled 6 DOF identification models including equivalent time delays characterize the BO 105 dynamics in the low and mid-frequency range up to about 13 rad/sec. This is satisfactory for application to handling-qualities and piloted simulations, which must be generally accurate over a wide spectrum frequencies from trim (zero frequency) and phugoid (low frequency) to the dominant transient responses of the longitudinal short-period and roll-subsidence modes (mid/high frequency). However, identification models intended for application to flight-control system design must be highly accurate in the crossover frequency range to exploit the maximum achievable performance from the helicopter. As a rule of thumb, dynamic modes with frequencies of 0.3 - 3.0 times the crossover frequency will contribute substantially to the closed-loop response. A typical high-bandwidth control system design for a modern combat helicopter will have a crossover frequency of about 6 rad/sec [6] thus indicating the need for an accurate identification in the frequency range of 2-18 rad/sec. Clearly, 6 DOF models are not sufficient for this purpose.

Six DOF models also proved to be inadequate for the design of the model-following control system for the DLR in-flight simulator BO 105-ATHeS [12]. The feed-forward controller basically is the inverse of the BO 105 state space model. Inverted time delays, however, result in time 'lead', requiring future measurements that are not available in an on-line process. On the other hand, the model must provide a highly accurate representation of the helicopter initial response. This requirement can no longer be met by 6 DOF models and clearly leads to the development and identification of extended models.

### 6.1 Model-Structure Determination

A satisfactory model is needed that will provide a good representation of the dynamic characteristics for frequencies up to about 3 Hz. This section examines the model-structure requirements for the roll response to lateral stick as an illustrative example. A 7-th order model of the roll angle response to lateral stick is selected as the "baseline model" that captures the key dynamics in the frequency-range for control system applications (2-18 rad/sec):

1. coupled roll/rotor regressing flapping dynamics (2nd order),
2. lead-lag/air resonance (2nd order),
3. dutch roll dynamics (2nd order),
4. roll angle integration (1st order),
5. actuator dynamics (equivalent time delay).

Dynamic inflow modes are not explicitly included in the above list, because of their small influence at this forward flight speed (40 m/s). (Implicit effects of inflow on the rotor modes are captured in the matching the frequency-response data.) The roll angle response to lateral stick transfer-function for the baseline model is then 4-th/7-th order:

$$\frac{\text{roll angle}}{\text{lateral stick}} = \frac{2.457[0.447, 3.2372][0.045, 14.94]e^{-0.0217s}}{(0)[0.317, 2.8560][0.021, 14.98][0.450, 13.142]}$$

The model parameters shown in the equation were obtained from a frequency response fit of Figure 16 from 1-30 rad/sec using 50 points. The frequency-response comparison with the data is seen in Figure 16 to characterize the dynamics accurately in the range of con-

cern. Also, accurate prediction of control system metrics such as crossover frequency and stability margins is crucial for control system design. The 45 degree phase margin crossover frequency for the baseline model is taken from the figure as  $\omega_c = 5.558$  rad/sec, which is within 5% of the data, and the baseline gain margin and closed-loop instability frequency matches the data. These results indicate that the baseline model is of sufficiently high order.

The transfer-function model indicates a highly coupled body-roll/rotor-flapping mode ( $\zeta = 0.45$ ,  $\omega = 13.14$  rad/sec) as is expected for the hingeless rotor system (high effective hinge offset) of the BO 105. Helicopters with low effective hinge offset rotors (or equivalently low flapping stiffness), such as some articulated systems, will generally exhibit two essentially decoupled first order modes;

1. body angular damping ( $L_p$ ,  $M_q$ ),
2. first-order rotor regressing.

The decoupled rotor mode is often modelled by an effective time delay, as was done herein, thus constituting the 6 DOF handling-qualities model. The degree of body/rotor coupling is determined by the flapping stiffness. The lead-lag mode is very lightly damped ( $\zeta = 0.0214$ ) due only to structural damping of the hingeless rotor. Significant roll/yaw coupling is apparent from the separation of the complex pole/zero combination of the dutch roll mode. Finally, the equivalent time delay of about 20 msec corresponds well to known control system hydraulics and linkage lags.

This section has shown that an appropriate model structure for high bandwidth identification should include the regressing rotor dynamics (1st order) and a second order lead-lag transfer function. These results are now used in an extended identification of the coupled body/rotor system.

## 6.2 Time-domain identification of extended models

In a first approach to extend the 6 DOF rigid body model two additional degrees of freedom, representing the regressing pitch and roll motion of the rotor tip path plane were added. This 8 DOF model is derived and explained in more detail in [13]. As the rotor is now explicitly included, the initial rotational acceleration response due to an input shows a first order system characteristic, which is more realistic than the immediate response of a 6 DOF model. Consequently, the 8 DOF model can be used without time delays and eliminates the associated problems. Figure 17 first compares the roll acceleration responses of

1. the 6 DOF model with time delays,
2. the extended 8 DOF model.

The improvement in the peak response is obvious. The still existing differences are due to the slightly damped lead-lag motion at a frequency of about 14 rad/sec. As no blade lagging data were available, this motion was modelled as a transfer function (second order for both numerator and denominator) for the lateral stick input. It was added to the 8 DOF model that now represented the rigid body, the first order rotor dynamics (flapping), and the lead-lag approximation. All coefficients were again identified, including the transfer function parameters. Figure 17 demonstrates that the oscillation in the roll acceleration response could be matched. It is also seen that the fit in the main peaks is unchanged, indicating that the lead-lag motion is widely decoupled from the flapping. This was also confirmed by the fact that the derivatives of the 8 DOF stayed almost the same. The identified transfer function coefficients agree almost perfectly with the above presented frequency-domain result for the lead-lag motion.

## Conclusions

Some of the main conclusions from an extensive evaluation of BO 105 flight test data, generated for system identification purposes, are:

1. An initial data consistency check proved to be extremely helpful in detecting instrumentation and calibration errors.
2. A consistent error model was identified for all of the maneuvers using the SMACK Kalman Filter program and the two-stage consistency check approach. This included small biases on  $p$  and  $q$ , small scale factors on  $\Phi$ ,  $\Theta$ , and  $u$ , and large scale factors on  $v$  and  $w$ . In addition, disturbances and time delays in the velocity measurements were

- removed leading to large improvements in the frequency-response-based identification and verification.
3. Both identification approaches, time- and frequency-domain, were able to determine a suitable 6 DOF rigid body model for handling qualities applications.
  4. The comparison of identified derivatives, eigenvalues, frequency responses and verification time histories shows good agreement. The solutions obtained individually by the two completely different techniques are very close. It certainly can be stated that larger improvements for 6 DOF models seem not to be necessary or possible, and that these models are useful for handling-qualities applications.
  5. Discrepancies still seen in the results can arise from the fact that the rotor dynamics are only represented by equivalent time delays. This relatively rough approximation is no longer suitable, when higher bandwidth requirements must be met. First approaches to extend the model by additional degrees of freedom for the rotor flapping mode and an approximation for the influence of the lead-lag coupling are promising for a further improvement of identification results.

## 8. References

- [1] Tischler, M.B. and Kaletka, J., *"Modeling XV-15 Tilt Rotor Aircraft Dynamics by Frequency and Time-Domain Identification Techniques,"* AGARD-CP-423, 1987, pp. 9-1 to 9-20
- [2] Jategaonkar, R. and Plaetschke, E. *"Maximum Likelihood Parameter Estimation from Flight Test Results for General Nonlinear Systems,"* DFVLR-FB 83-14, 1983
- [3] Tischler, M.B., *"Frequency-Response Identification of XV-15 Tilt-Rotor Aircraft Dynamics,"* NASA TM 89428, ARMY TM 87-A-2, May 1987.
- [4] Tischler, M.B., *"Advancements in Frequency-Domain Methods for Rotorcraft System Identification,"* 2nd International Conference on Rotorcraft Basic Research, University of Maryland, College Park, MD, 16-18 Feb 1988.
- [5] Tischler, M.B., Fletcher J.W., Diekmann, V.L., Williams, R.A., and Cason, R.W., *"Demonstration of Frequency-Sweep Test Technique Using a Bell-214-ST Helicopter,"* NASA TM 89422, ARMY TM 87-A-1, April 1987.
- [6] Tischler, M.B., Fletcher, J.W., Morris, P.M., and Tucker, G.T., *"Application of Flight Control System Methods to an Advanced Combat Rotorcraft,"* Royal Aeronautical Society International Conference on Helicopter Handling Qualities and Control, London, UK., 15-17 Nov., 1988 (also NASA TM101054, July 1989).
- [7] Holland, R., *"Digital Processing of Flight Test Data of a Helicopter without Using Anti Aliasing Filters,"* ESA Translation from DFVLR-Mitt. 87-12, ESA-TT-1094, 1987.
- [8] Kaletka, J., *"Practical Aspects of Helicopter Parameter Identification,"* AIAA CP 849, 1984, pp. 112-122, AIAA No. 84-2081
- [9] Bach, Ralph E., Jr., *"State Estimation Applications in Aircraft Flight-Data Analysis (A User's Manual for SMACK),"* NASA Ames Research Center, May, 1984.
- [10] Chen, R.T.N., and Tischler, M.B., *"The Role of Modeling and Flight Testing in Rotorcraft Parameter Identification,"* Vertica Vol 11, No. 4, pp 819-847, 1987.
- [11] Kaletka, J., *"Evaluation of the Helicopter Low Airspeed System Lasse,"* Seventh European Rotorcraft and Powered Lift Aircraft Forum, Garmisch-Partenkirchen, 1981
- [12] Pausder, H.-J., von Grünhagen, W., Henschel, F. and Zöllner, M., *"Realization Aspects of Digital Control Systems for Helicopter,"* Conference on 'Helicopter Handling Qualities and Control', London UK, Nov. 15-17, 1988
- [13] Kaletka, J. and von Grünhagen, W. *"Identification of mathematical derivative models for the design of a model following control system" Paper presented at the 45th Annual AHS Forum, Boston MA, 1989*

Event	$\rho_{bias}$	$q_{bias}$	$\Phi_{s.f.}$	$\Theta_{s.f.}$	$u_{s.f.}$	$v_{s.f.}$	$w_{s.f.}$
1	0.1000	0.1119	1.0290	1.0530	0.9698	0.6923	0.8878
2	0.0953	0.1113	1.0250	1.0550	1.0270	1.0830	0.9950
3	0.0740	0.0969	1.0290	1.0440	0.9698	0.5385	0.9095
4	0.0882	0.0884	1.0180	1.0560	1.0300	*1.7120	1.1620
5	*0.0356	0.0724	1.0050	1.0110	1.0560	0.6859	0.7776
6	0.0400	0.0927	1.0010	*0.8989	1.1210	0.8957	0.7159
7	0.1141	0.1013	1.0330	1.0710	0.9632	1.0290	0.9057
8	0.1201	0.1021	1.0240	1.0630	1.0330	0.8521	0.9484
9	0.0518	0.1081	1.0440	*0.9107	1.0510	1.2350	0.9271
10	0.0628	0.0881	1.0440	1.0430	0.9342	0.4641	0.8036
11	0.0552	0.0720	1.0200	0.9816	0.9802	1.0250	0.8329
12	0.1183	0.0976	1.0200	1.0310	0.9763	0.4251	0.8149
13	0.0847	0.0926	1.0250	1.0450	0.9794	0.5250	0.9081
14	0.1203	0.0830	0.9893	1.0080	*1.1930	0.7835	0.8749
15	0.0621	0.1267	0.9949	0.9844	1.0240	0.7884	0.9274
16	0.0506	0.0715	1.0220	1.0050	*1.1340	0.8326	0.6891
17	0.1226	*0.1677	1.0090	1.0300	1.0050	*1.5290	0.9676
18	0.0795	0.0999	1.0230	1.0440	0.9508	0.5150	0.9308
19	0.0772	0.1155	1.0370	0.9906	0.9637	0.8658	0.9102
20	0.0947	0.1139	1.0260	1.0450	0.9285	0.6212	0.9835
21	0.0655	0.0990	1.0290	1.0270	0.8896	*1.5780	0.8174
22	0.0864	0.1032	1.0230	1.0500	0.9173	0.5911	0.9815
23	0.0828	0.0874	1.0140	1.0580	1.0190	0.5343	0.9924
24	0.0865	0.0932	1.0200	1.0600	0.9937	0.8587	1.0860
25	0.0861	0.1102	1.0280	1.0560	0.9293	0.3688	0.9783
26	0.0997	*0.1434	1.0050	1.0130	0.9901	1.0140	0.7405
27	0.0806	0.1263	1.0250	1.0410	0.9290	1.3490	1.0840
28	0.0786	*0.1440	1.0200	1.0420	0.9277	1.1530	1.0680
29	0.0725	0.0938	1.0230	1.0460	0.9928	1.0330	1.0200
30	0.0938	0.0906	1.0210	1.0560	0.9241	1.1650	0.9633
31	0.0712	0.0786	0.9999	0.9741	0.9119	0.9095	*0.5098
32	0.0781	0.0855	1.0200	1.0460	0.9918	0.7170	1.0140
33	0.0624	0.1060	1.0070	1.0530	0.9192	0.5986	0.8892
34	0.0750	0.0858	1.0130	1.0360	0.9648	0.7334	0.8288
35	0.0860	0.0799	1.0160	1.0230	1.0160	0.6604	0.8065
36	0.0962	0.0970	1.0200	1.0450	0.9646	0.6643	0.9330
37	0.0423	0.1155	1.0410	1.0330	1.0490	0.7954	0.9713
38	0.1166	0.0963	1.0220	1.0700	0.9859	0.9735	1.0860
39	0.0784	0.1031	1.0270	1.0530	0.9556	0.6338	0.9361
40	0.0830	0.1042	1.0170	1.0370	0.9812	0.7570	0.9460
41	0.0527	0.0941	1.0250	0.9826	0.9840	0.7037	0.8668
42	0.0705	0.0924	1.0040	0.9965	0.9700	0.7900	0.8900
43	0.0723	0.0925	1.0290	1.0240	0.8692	0.5367	0.8589
44	0.0697	0.0926	1.0100	0.9991	0.9075	0.5293	0.9129
45	0.0671	0.0933	1.0120	1.0120	*0.8148	0.7207	0.7855
46	0.0709	0.0922	1.0130	1.0270	0.8989	0.6637	0.8232
47	0.0897	0.0951	1.0100	1.0480	1.0260	0.6411	*1.3010
48	0.1058	0.1030	1.0240	1.0300	1.0770	0.9024	1.1050
49	0.0861	0.0897	1.0340	1.0740	0.9053	0.5816	0.7803
50	0.0725	0.0938	1.0500	1.0240	0.8453	0.4473	0.6598
51	0.0697	0.0932	1.0180	1.0380	1.0400	0.8678	0.7768
52	0.1068	0.0940	0.9973	1.0610	*1.1400	0.5769	0.7581
Mean	0.0808	0.0997	1.0199	1.0290	0.9912	0.8105	0.9046
S.D.	0.0210	0.0178	0.0126	0.0352	0.0731	0.2954	0.1352

estimate = (measurement - bias) / scale factor

\* indicates greater than two standard deviations away from mean

Table 1. Table of biases and scale factors determined with SMACK

	Time-domain	Freq.-domain
Derivative	Param Value	Param Value
$L_p$	-8.501	-11.132
$L_q$	3.037	4.371
$L_r$	0.410	0.000 +
$L_u$	-0.081	-0.094
$L_v$	-0.271	-0.324
$L_w$	0.116	0.265
$M_p$	-0.419	-1.037
$M_q$	-3.496	-5.108
$M_r$	-0.117	-0.290
$M_u$	0.029	0.000 +
$M_v$	0.048	0.063
$M_w$	0.053	0.113
$N_p$	-1.057	-0.665
$N_q$	0.809	4.796
$N_r$	-0.858	-1.292
$N_u$	0.000 †	-0.033
$N_v$	0.117	0.089
$N_w$	0.034	-0.081
$X_p$	0.000 †	0.773
$X_q$	0.000 †	2.068
$X_r$	0.000 †	0.607
$X_u$	-0.059	-0.047
$X_v$	0.000 †	0.000 +
$X_w$	0.036	-0.044
$Y_p$	0.000 †	-3.794
$Y_q$	0.000 †	3.037
$Y_r$	1.332	0.932
$Y_u$	0.000 †	0.000 +
$Y_v$	-0.170	-0.287
$Y_w$	0.000 †	0.000 +
$Z_p$	0.000 †	3.172
$Z_q$	5.012	9.947
$Z_r$	0.000 †	0.000 +
$Z_u$	0.014	0.152
$Z_v$	0.000 †	0.000 +
$Z_w$	-0.998	-1.195

	Time-domain	Freq.-domain
Derivative	Param Value	Param Value
$L_{\delta_{lat}}$	0.185	0.216
$L_{\delta_{col}}$	0.032	0.059
$L_{\delta_{len}}$	0.024	0.070
$L_{\delta_{ped}}$	-0.028	-0.023
$M_{\delta_{lat}}$	-0.009	0.000 +
$M_{\delta_{col}}$	0.057	0.077
$M_{\delta_{len}}$	0.093	0.112
$M_{\delta_{ped}}$	0.000 †	0.010
$N_{\delta_{lat}}$	0.026	0.033
$N_{\delta_{col}}$	0.000	-0.038
$N_{\delta_{len}}$	0.000 †	-0.063
$N_{\delta_{ped}}$	0.049	0.054
$X_{\delta_{lat}}$	0.000 †	0.000 +
$X_{\delta_{col}}$	0.000 †	-0.043
$X_{\delta_{len}}$	-0.028	-0.067
$X_{\delta_{ped}}$	0.000 †	0.000 +
$Y_{\delta_{lat}}$	0.003	0.091
$Y_{\delta_{col}}$	0.000 †	0.000 +
$Y_{\delta_{len}}$	0.000 †	0.000 +
$Y_{\delta_{ped}}$	-0.011	0.000 +
$Z_{\delta_{lat}}$	0.000 †	0.000 +
$Z_{\delta_{col}}$	-0.349	-0.365
$Z_{\delta_{len}}$	-0.303	-0.187
$Z_{\delta_{ped}}$	0.000 †	0.000 +
$\tau_{\delta_{lat}}$	0.060	0.079
$\tau_{\delta_{col}}$	0.040	0.183
$\tau_{\delta_{len}}$	0.100	0.124
$\tau_{\delta_{ped}}$	0.040	0.048

† Eliminated from model structure

+ Eliminated during model structure determination

Table 2. BO 108 Identification results.

	dlon	dlat	dped	dcol
u	*	*	*	*
v		*	*	
w	*	*		*
p	*	*	*	*
q	*	*	*	*
r	*	*	*	
$a_x$	*			
$a_y$	*	*	*	
$a_z$	*			*

State names:

u v w p q r  $\phi$   $\theta$

Output names:

u v w p q r  $a_x$   $a_y$   $a_z$

Control names:

dlon dlat dped dcol

Number of frequencies: 19

Weight: 7.570 deg-error/dB-error

\* - indicates an input/output frequency-response that is included in the identification cost function

Table 3. BO 105 Set-up for frequency-domain identification

Motion	DLR	US
	$[\zeta, \Omega_0]$	$[\zeta, \Omega_0]$
Phygoid	$[-0.15, 0.33]$	$[-0.33, 0.32]$
Dutch Roll	$[+0.14, 2.50]$	$[+0.19, 2.65]$
	$\left(\frac{1}{T}\right)$	$\left(\frac{1}{T}\right)$
Roll	(8.49)	(10.76)
Pitch	(4.36)	(6.96)
Pitch	(0.60)	(0.51)
Spiral	(0.02)	(0.03)

Table 4. Comparison of BO 105 eigenvalues

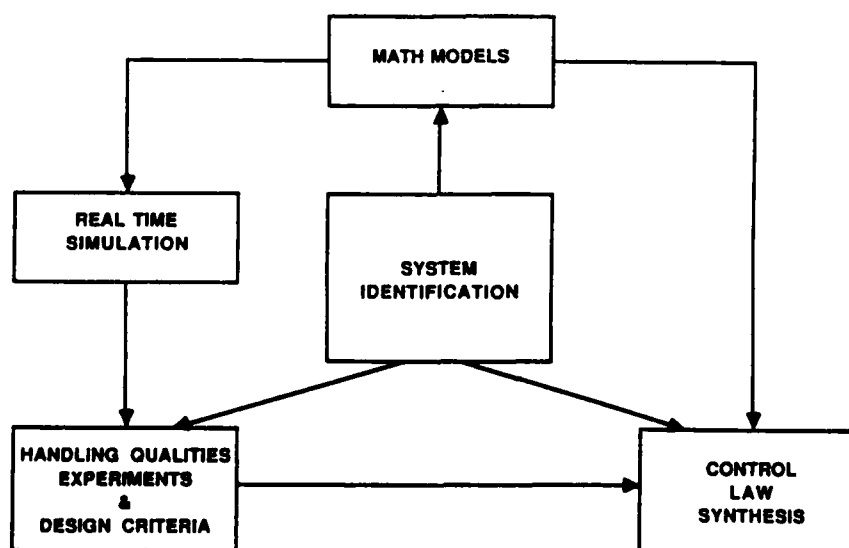


Figure 1. The role of system identification

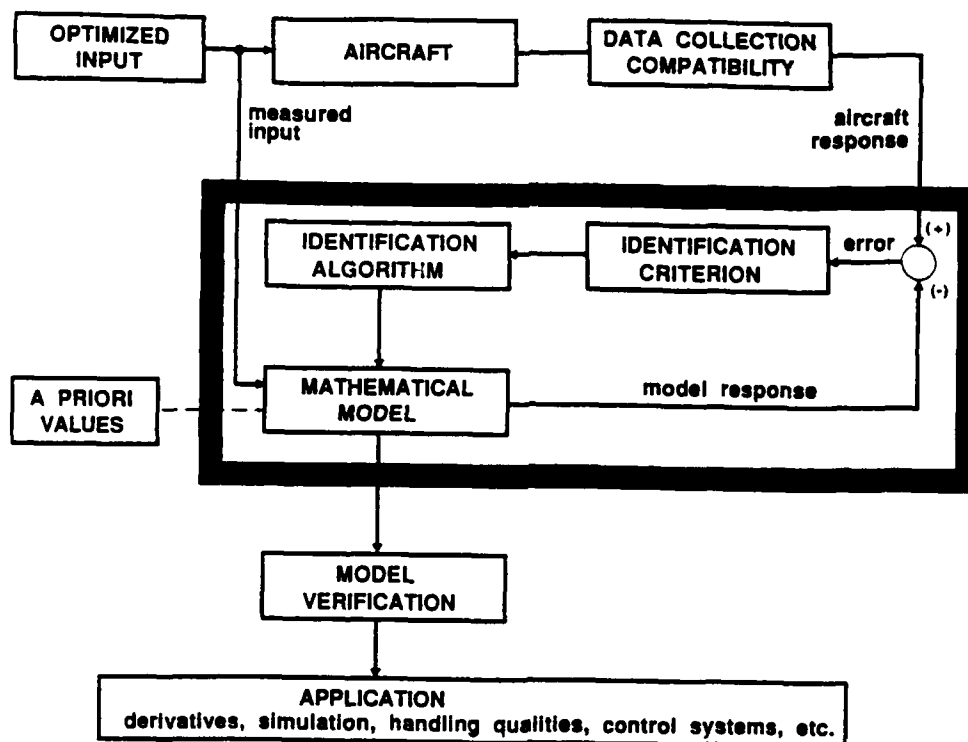


Figure 2. Time-domain system identification method

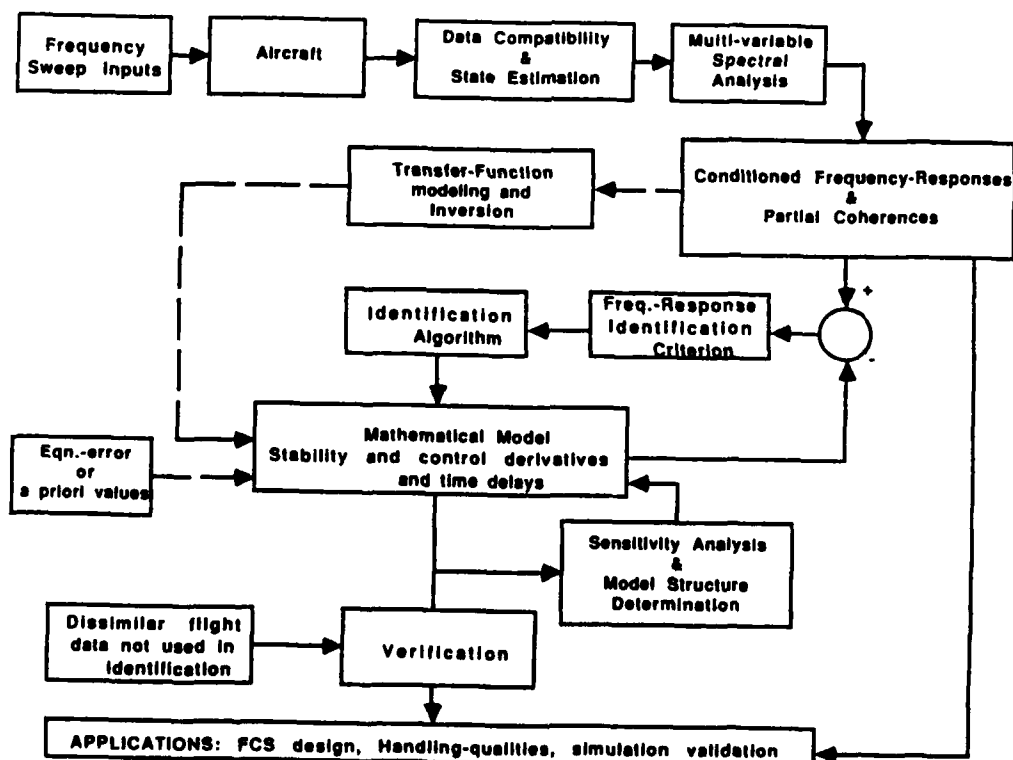


Figure 3. Frequency-domain identification procedure

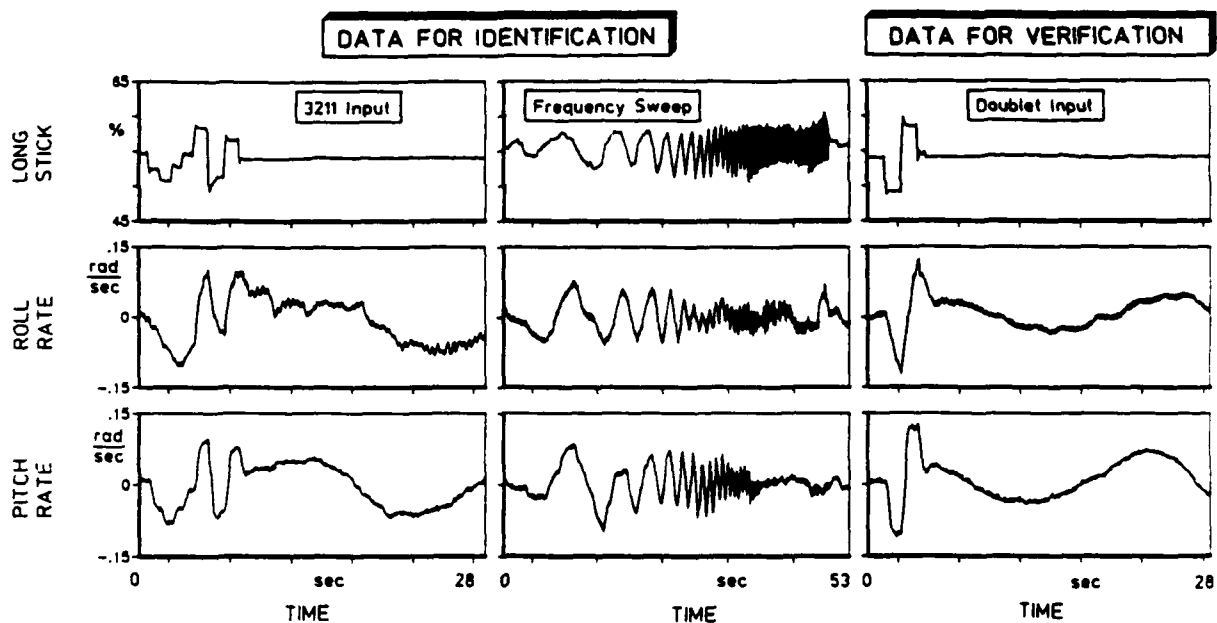


Figure 4. Representative flight test data with 3211 and frequency sweep inputs

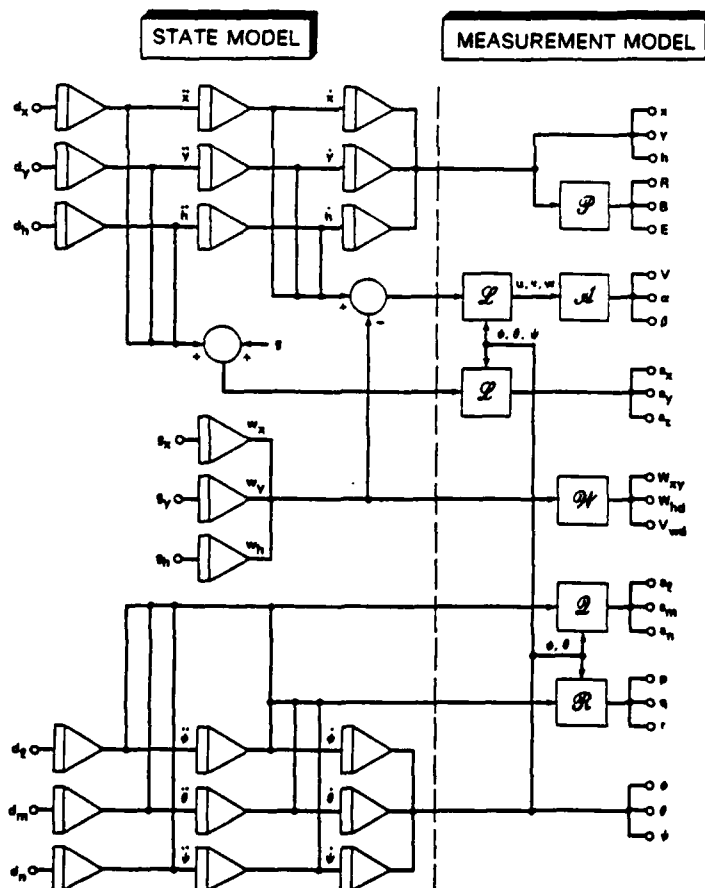


Figure 5. State and measurement models used by SMACK

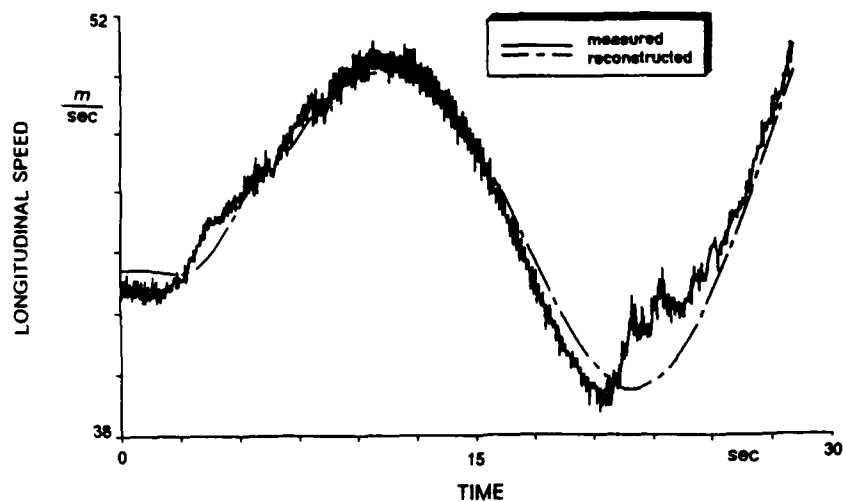


Figure 6. Comparison of measured and reconstructed longitudinal velocity signals

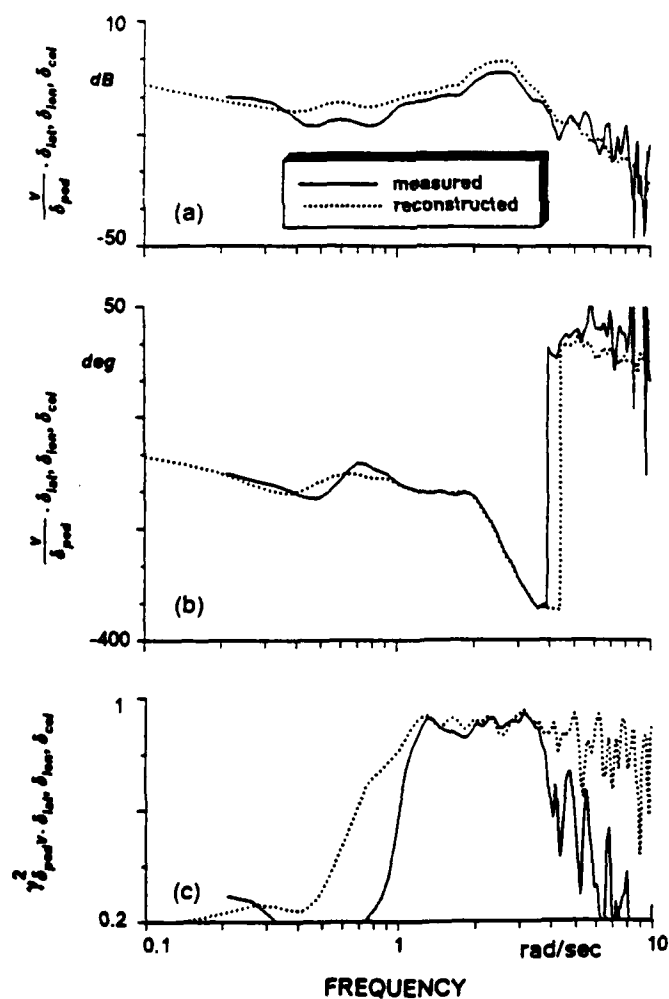


Figure 7. Comparison of lateral speed/pedal conditioned frequency responses using measured and reconstructed lateral velocity signals (a = Magnitude b = Phase c = Coherence)

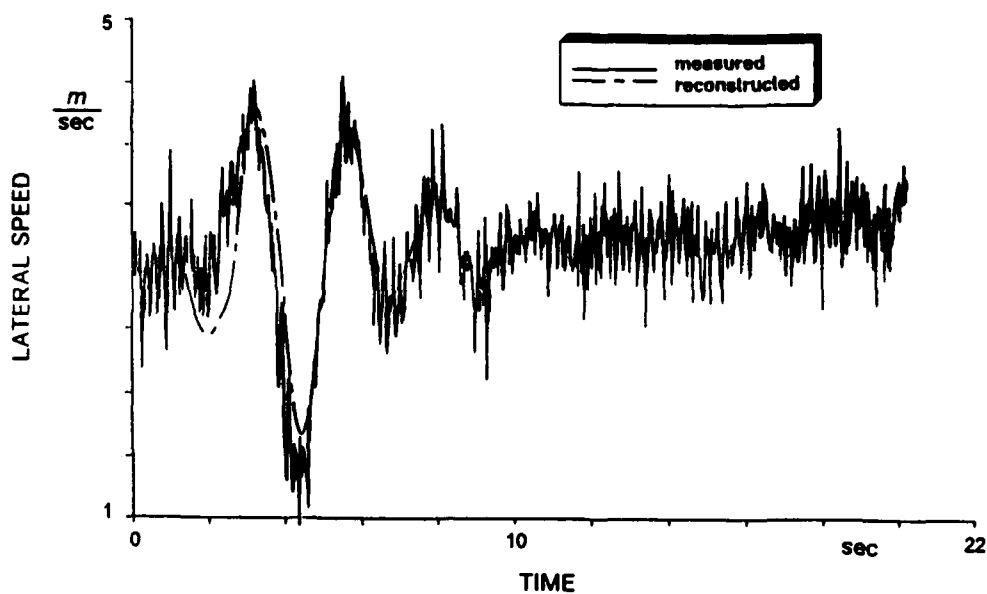


Figure 8. Illustration of phase shift in lateral velocity signal

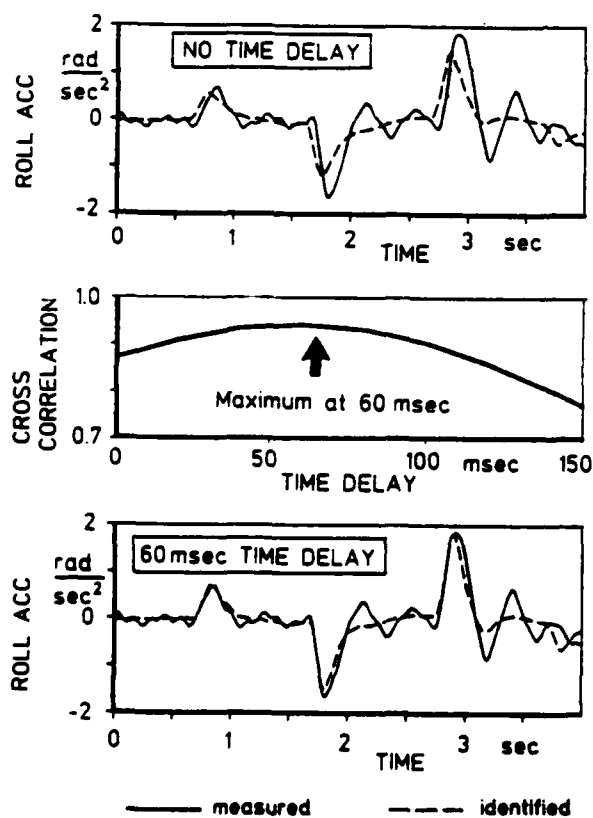


Figure 9. Determination of the equivalent time delay for the roll acceleration response

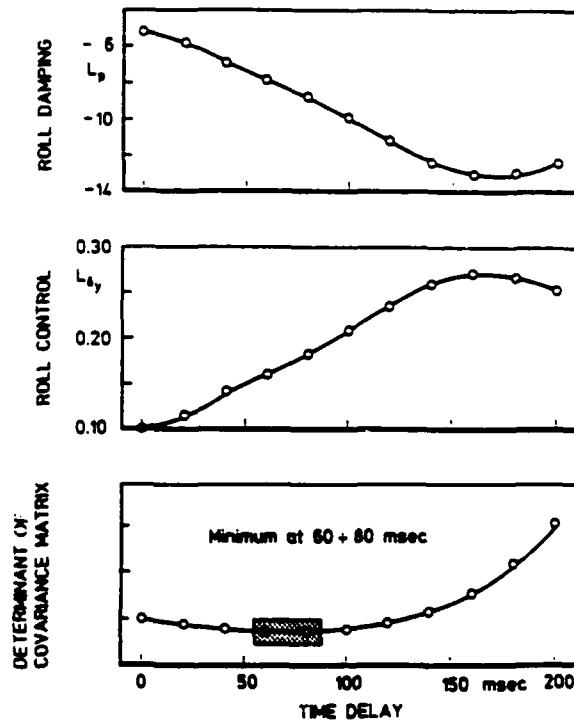


Figure 10. Influence of equivalent time delays on identification results

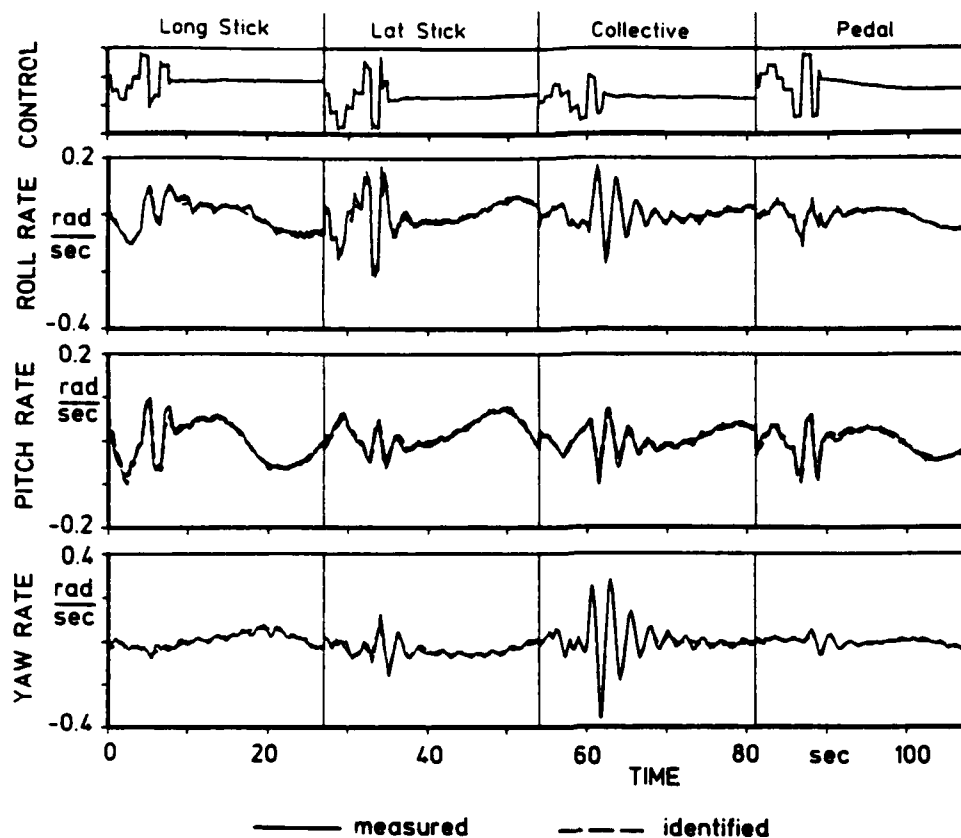


Figure 11. Comparison of time histories for the identified 6 DOF model (Time-domain result)

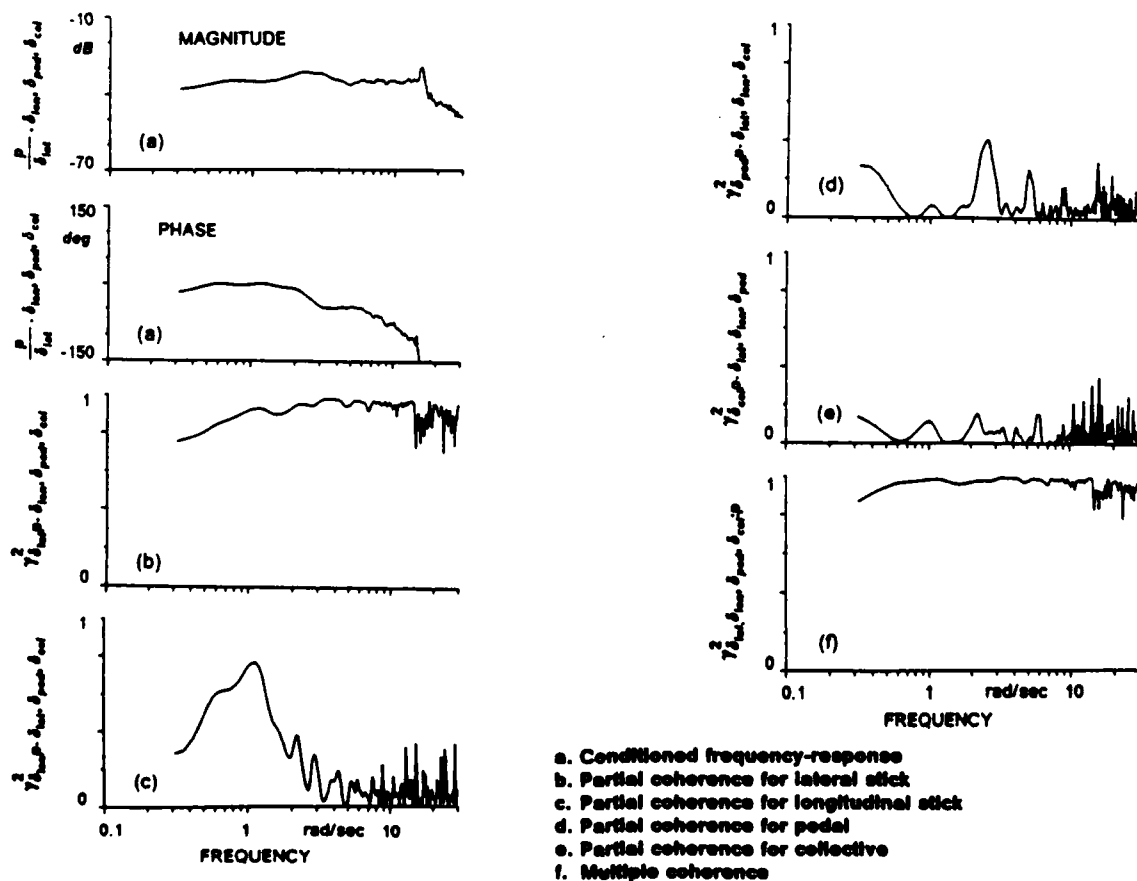


Figure 12. Identification of roll rate response to lateral stick

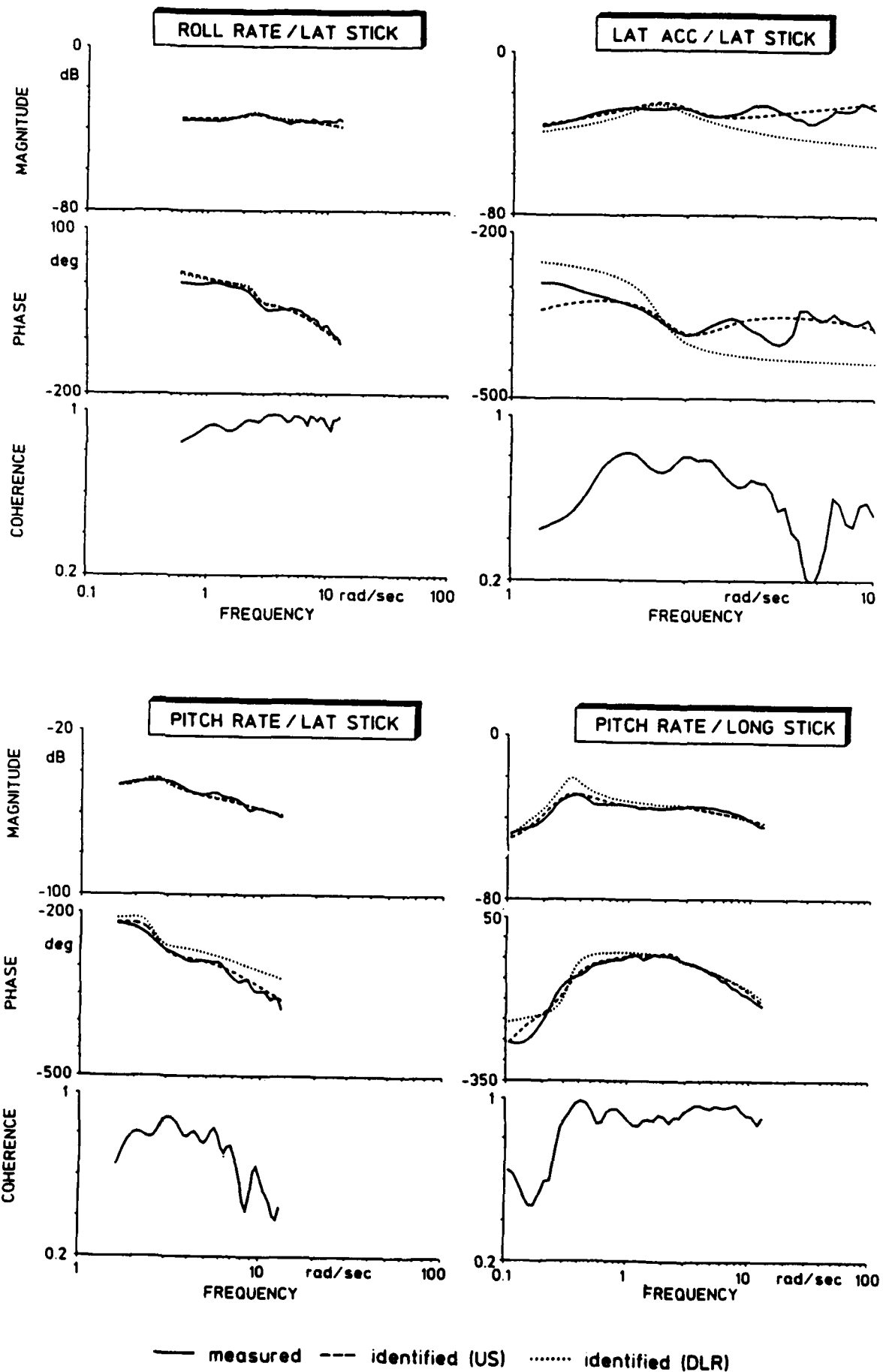


Figure 13. Comparison of flight data and identified model frequency responses

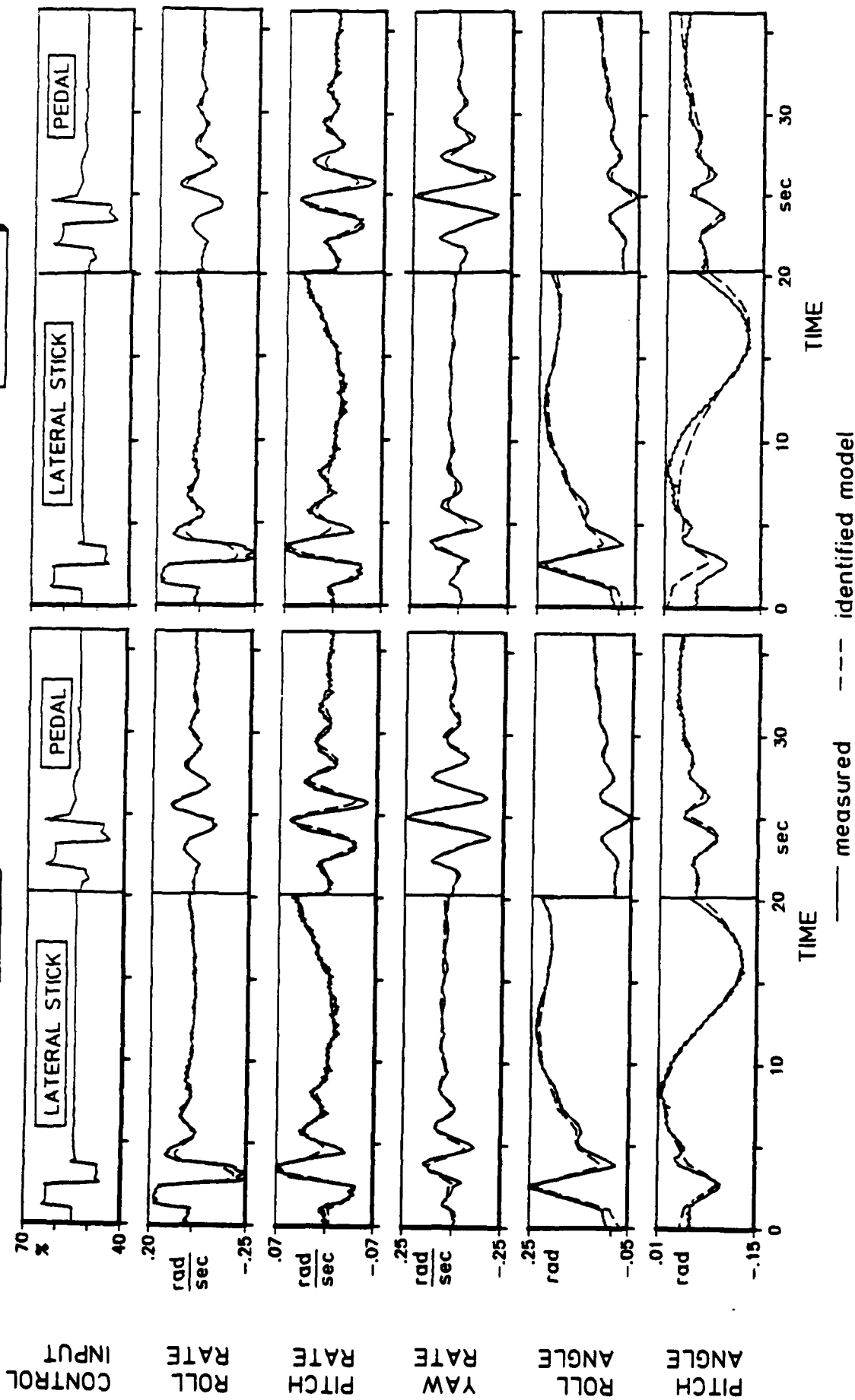
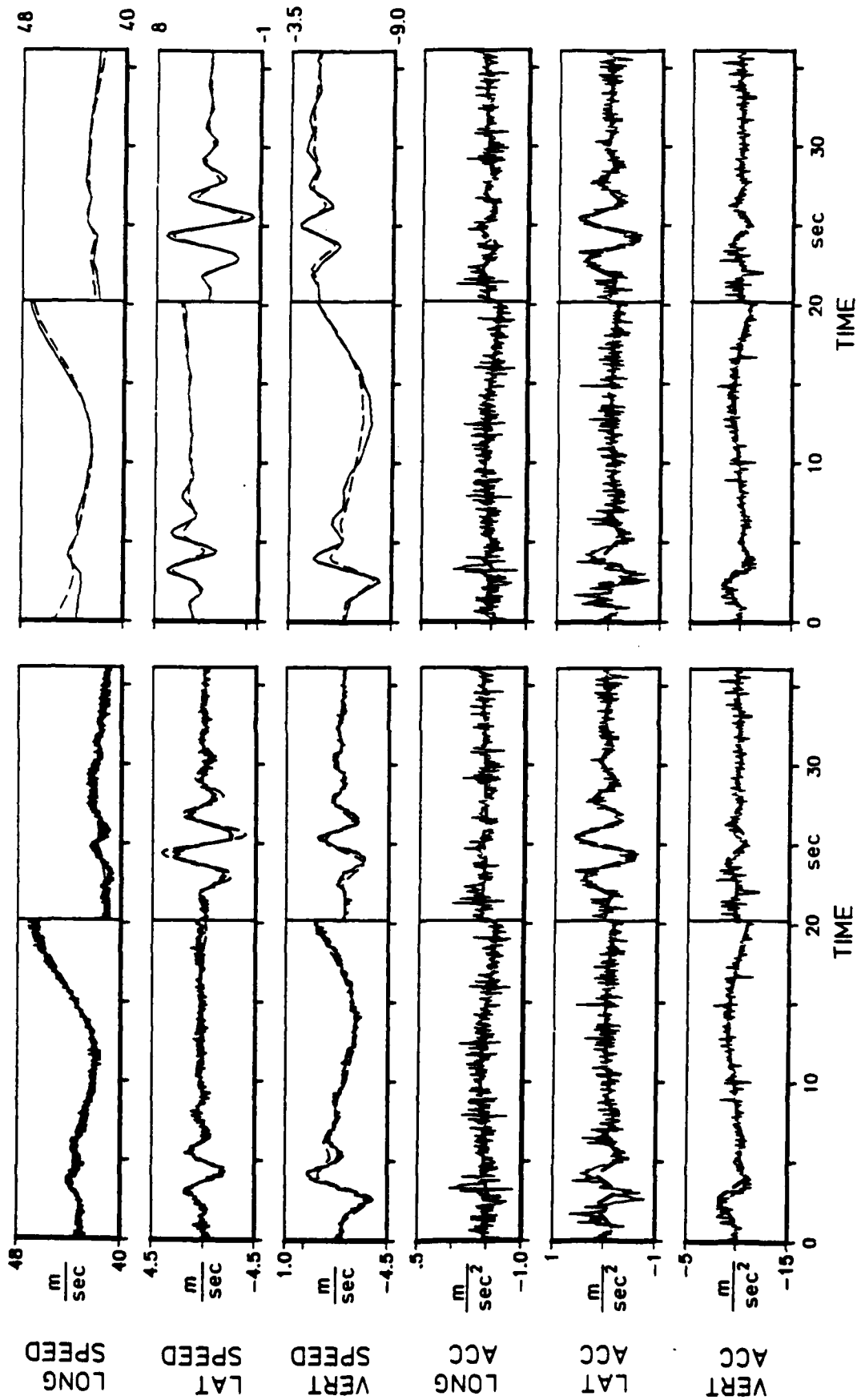


Figure 14. Verification of identified models

DLR

US ARMY



— measured  
--- identified or reconstructed

Figure 14. Verification of Identified models -continued-

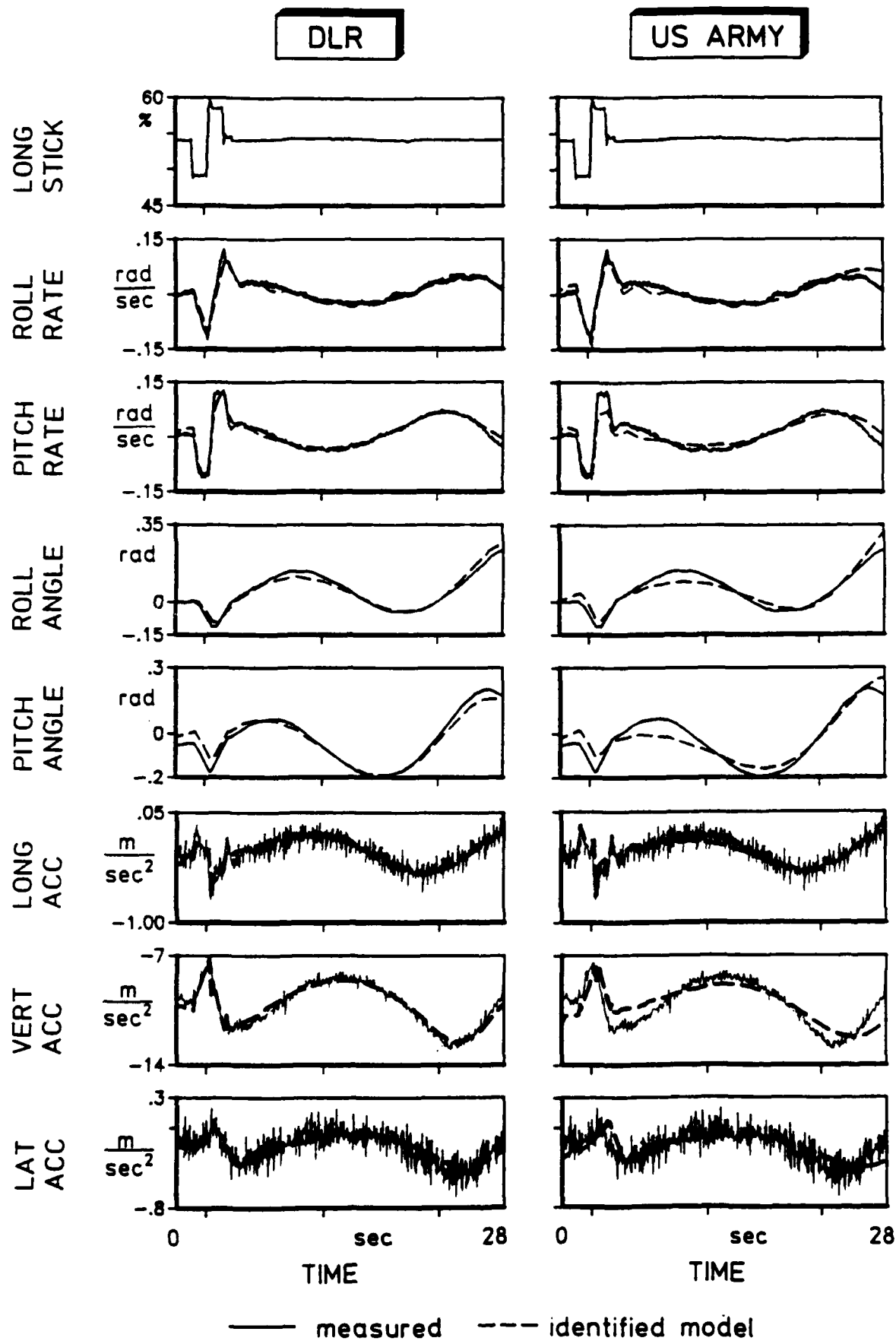


Figure 15. Verification of Identified models

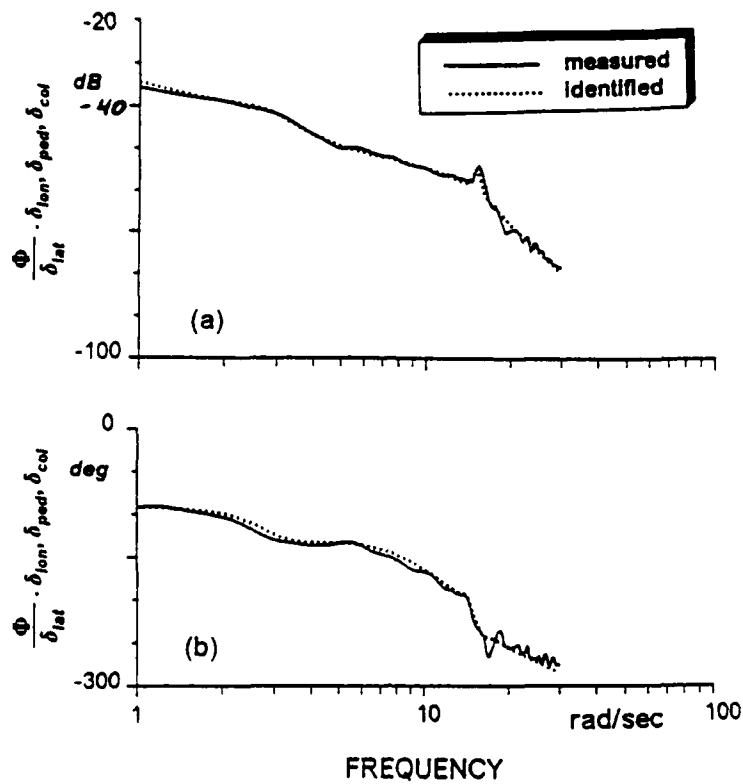


Figure 16. Comparison of baseline model (7-th order) and flight data for roll attitude response to lateral stick (a = Magnitude b = Phase)

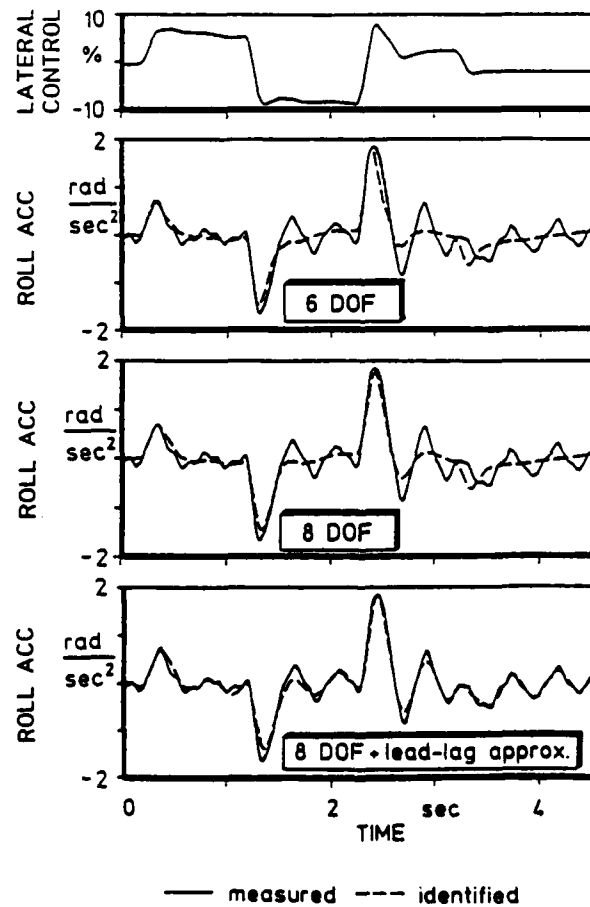


Figure 17. Comparison between the initial responses of the 6 DOF and extended models